

A comparative study on the acoustic behaviour of free-standing curved and flat single panel screens in an open-plan enclosed environment

| | |
|---------------|--|
| Item Type | Conference contribution |
| Authors | Arjunan, Arun;Foteinou, Aglaia |
| Citation | INTER-NOISE and NOISE-CON Congress and Conference Proceedings, InterNoise17, Hong Kong CHINA, pages 1996-2998, pp. 2359-2369(11) |
| Publisher | Institute of Noise Control Engineering |
| Journal | INTER-NOISE and NOISE-CON Congress and Conference Proceedings |
| Rights | Attribution-NonCommercial-NoDerivs 3.0 United States |
| Download date | 2026-04-13 23:28:06 |
| License | http://creativecommons.org/licenses/by-nc-nd/3.0/us/ |
| License | https://creativecommons.org/licenses/by-nc-nd/4.0/ |
| Link to Item | http://hdl.handle.net/2436/621937 |



A comparative study on the acoustic behaviour of free-standing curved and flat single panel screens in an open-plan enclosed environment

Arun ARJUNAN¹; Aglaia FOTEINOU¹

¹ University of Wolverhampton, United Kingdom

ABSTRACT

Free-standing flat screen partitions are commonly used in open-plan environments to improve the visual and acoustic privacy of employees and to differentiate individual work spaces. Acoustic behaviour of flat screen single leaf barriers under free-field conditions have been extensively studied over the past years. However, the behaviour of such structures in enclosed spaces are not fully investigated; thus, missing any opportunities for geometrical improvements, such as damping due to added curvature. Curved structures are known to exhibit different stiffness and acoustic reflection properties compared to flat structures of similar global dimensions. Consequently, this work is an initial attempt to understand the acoustic performance of free-standing curved screens in comparison with flat screens of similar global dimensions within in an open-plan but enclosed environment. The acoustic performances of four different barrier designs are studied experimentally within an enclosure. The Sound Pressure Level (SPL) after introducing these barriers under 'White' and 'Pink' noises are analysed for a frequency range of 100 Hz and 16 kHz at one-third-octave bands. The single number equivalent LA_{eq} values are also compared for each of the four cases to quantify overall performance improvements. Furthermore, a 2D vibro-acoustic simulation model capable of Fluid-Structure Interaction (FSI) is developed using the Finite Element Method (FEM) as part of this study. The numerical model was extended to analyse SPL of an open-plan enclosure before and after insertion of simple flat barrier. The simulation model presented is validated in comparison with experimental tests data complying relevant standards. This in turn can aid in the development of acoustically efficient free-standing partitions for open-plan enclosures.

Keywords: Open-plan Enclosure, Sound Pressure Level, I-INCE Classification of Subjects Number(s): 31.2

1. INTRODUCTION

The provision of aural comfort within an open-plan enclosed space is one of the major tasks for acoustic researchers and noise control engineers (1). With the widening use of open-plan offices the performance of indoor noise barriers along with their design prediction are becomingly increasingly important. One of the key features of open-plan offices is the absence of full height partitions for isolating workers from one another. Consequently, free standing screens are often used as partitions to create individual workplaces, which are referred to as cubicles. However, with this come acoustic issues such as increased noise and decreased speech privacy.

The performance of various types of noise barriers in the free-field condition has been widely studied (2-4). In these types of analyses, only ground reflections and diffraction around the barrier edges are considered and reflection from walls or ceilings omitted. Huang *et al.* (5) investigated the performance of indoor active noise barriers using 2D simulation and suggested possible improvements in Insertion Loss (IL). The improved insulation was achieved using an active noise reduction technique coupled to an existing noise barrier. Lin *et al.* (6) attached a vibration absorber to one side of the panel and discussed its effects by means of a simple one-degree of freedom model. Mu *et al.* (7) studied the effect of applying micro-perforation to the transmission side of the panel and confirmed

¹ a.arjunan@wlv.ac.uk

possible improvements for sound reduction.

On the measurement side, a simplified chart and expression for estimating the acoustic performance of a long barrier under free field conditions have been put forwarded by researchers (2,3). Although various other analytical methods have been proposed (8,9); Maekawa's chart (3) and the theory of Kurze (2) still remain widely used by engineering for outdoor applications. A comprehensive review on the existing formulae for predicting the Insertion Loss (IL) of sound barriers under free field conditions were carried out by Li and Wong (10).

In contrast, the influences of the geometry on the acoustic performance of barriers enclosed spaces are yet to be fully understood. The acoustic performance of a barrier in an enclosure is complex due to the existence of non-uniform reflections from structural boundaries. Given the shortcomings of previous studies in this area and the fact that the extended development of theoretical approach has been largely neglected; this research aims to study the acoustic performance of barriers inside an enclosed space using both experimental and Finite Element (FE) methods. Using the data, attempts has been made to conduct a more in-depth analysis on to the influence of barrier curvature.

For most plate like building structures such as walls, doors and windows the acoustic assessment criteria have been widely studied and various recommendations put forwarded (11-19). Overall, the literature shows that the acoustic insulation of such structures is highly dependent on the material, number of layers, mass, and stiffness (16). Despite the existing literature on building elements, there has been no published literature on the effect of curved geometry on free standing barriers. Consequently, this work attempts to investigate the effect of curvature on the acoustic insulation of free standing barriers in an enclosed space. The study will also investigate the feasibility of predicting the acoustic performance using and FE acoustic model featuring Fluid-Structure Interaction (FSI).

The lack of literature on the FE method to predict the acoustic insulation of building components has been reported in various publications (16,20,21). The reason for this is the complexity of the dynamic behaviour along with a vast number of variable parameters that need considering. Some of these parameters are difficult to evaluate, and have a considerable influence on the refinement of simulation models. In particular, it is difficult to include the effect of mechanical connections, non-uniformly disturbed mechanical damping mechanisms, and structure-acoustic coupling.

Accordingly, the presented study investigates the influence of geometrical curving on the acoustic performance of free standing partitions within an enclosed environment. There are no published literatures in this direction. A total of four different cases are analysed through experimental tests carried out at one-third-octave bands for a frequency range of 100 Hz to 16 kHz. Furthermore, a 2D vibro-acoustic model is also developed to visualise the spatial acoustic pressure for an enclosure with and without a flat panel barrier. The results of this study are expected to provide a better understanding on the acoustic performance of free-standing single panel structures in enclosed environments.

2. METHODOLOGY

2.1 Experimental Data Acquisition

The Sound Pressure Level (SPL) produced by a sound source was measured for a total of four different barriers as shown in Figure 1. The barriers were placed inside a rectangular enclosed space, which was an empty room of dimensions $20 \times 4.3 \times 3.8$ m. The room has masonry and plastered walls, a suspended tile ceiling and a carpeted floor.

The barriers were 1.5 m high and had a gauge thickness of 0.035 m. They were constructed out of 15 mm Melamine Faced Chipboard (MFC) core sandwiched between 9 mm polyurethane foam on each side before being covered in 1mm layer of flock. The barriers were mounted vertically as free standing with the support of metal clamps placed every 0.75m.

The experimental test setup was as shown in Fig. 2. The sound source was a BSWA OS003 Omni unit comprising 12 loudspeakers assembled evenly on a 280mm diameter sphere. The sound source was in compliance with ISO 140-3 (GB/T 19889.3), ISO 140-4 (GB/T 19889.4) and ISO 3382-3 (22,23) with a frequency range of 100 Hz to 16 kHz.

An omnidirectional sound source was deemed suitable for this project considering people in an open-plan office can speak in any direction. The sound source was mounted on a tripod and placed at 1m from the floor and the barrier coinciding with the centre of the width of the room. The sound source was connected to a SWA100 power amplifier. VA Lab 4 was used as a noise generator for Pink and White noise and was linked to the amplifier via the MC3242, 4 channel data acquisition card.

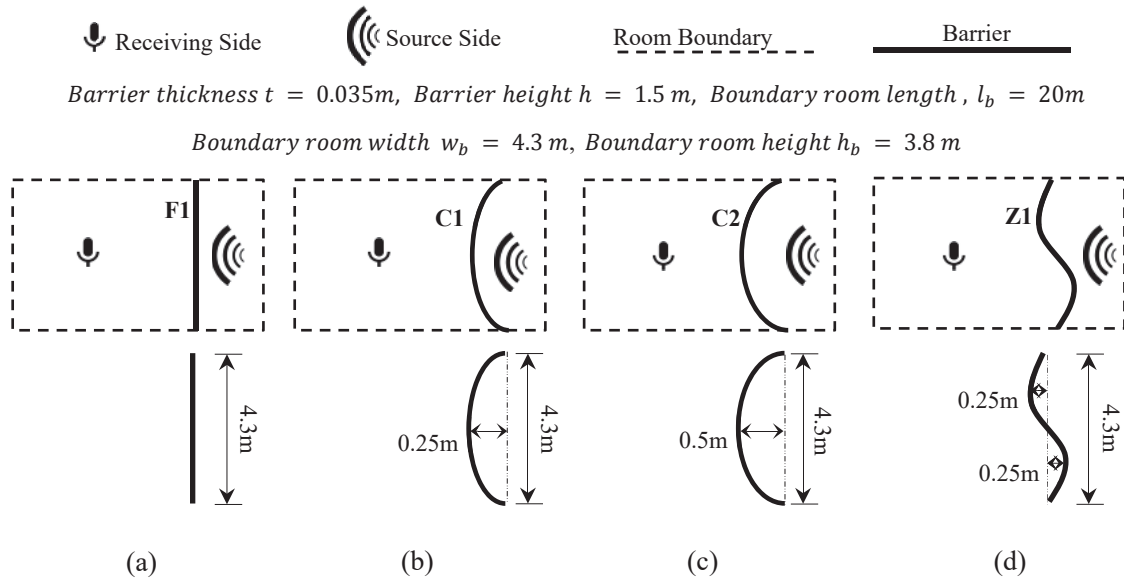


Figure 1 – Four types of barriers considered, (a) ‘F1’ flat barrier, (b) ‘C1’ 0.25m curved barrier, (c) ‘C2’ 0.5m curved barrier and (d) ‘Z1’ zigzag barrier.

The microphone to measure the SPL was placed along the centre width of the room coinciding with the height of the sound source. A total of six measurement positions were used; R1 was placed at a distance of 1m from the barrier and consequent microphones R2 to R6 at a distance of 2 m along the centre width of the room one after the other. The microphones used were omnidirectional and had a frequency range of 6.3 Hz to 20 kHz complying with class 1 IEC 61672-1 regulations (24). The microphones were connected to a class 1 compliant sound level meter made by Cirrus Research plc.

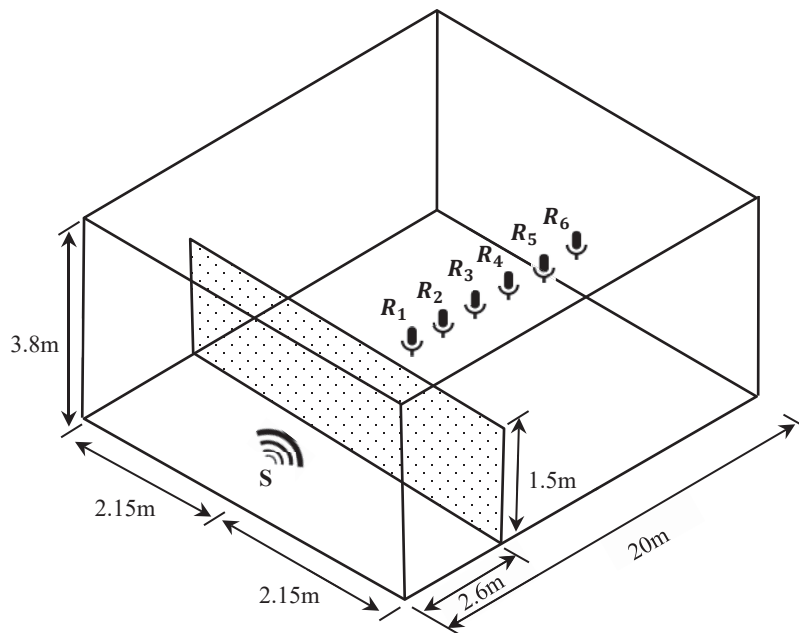


Figure 2 – Experimental test setup for SPL measurements

Using the experimental setup shown in Figure 2, SPL was measured for a total of five cases; (1) no barrier in room, (2) using plain barrier F1, (3) using curved barrier C1, (4) using curved barrier C2 and (5) using zigzag barrier Z1. For each case measurement were carried for both White and Pink noise source. The test conditions were kept constant throughout the measurements and the only change were the type of barriers used.

2.2 Finite Element Analysis

This study employs a 2D FEM by solving the wave equation; a full-scale 3D model was not practical at this stage due to computational complexity of the problem. For the presented acoustic problem, the structural dynamics equation needs to be considered along with Navier-Stokes equations of fluid momentum and the flow continuity equation (25). The Navier-Stokes and flow continuity equations were simplified to get the acoustic wave equation:

$$\frac{1}{c^2} \frac{\partial^2 P}{\partial t^2} - \nabla^2 = 0 \quad (1)$$

Where c is the sonic velocity, P is the acoustic pressure and t is the time. Accordingly, the harmonically varying pressure P can be defined as $\bar{P}e^{j\omega t}$, where \bar{P} is the pressure amplitude. Once the acoustic pressure is obtained, the sound level is calculated using equation (2).

$$L_p = 10 \log \frac{P}{20 \times 10^{-6}} \quad (2)$$

The 2D FE meshed model for the vibro-acoustic analysis is shown in Figure 3. Where, 'a' shows the FSI elements for the brick wall, 'b' shows fluid elements representing air, 'c' shows the FSI elements interaction with tiled ceiling, 'd' shows the structural element representing the barrier, 'e' shows the interface element representing FSI between barrier and air and 'f' shows the FSI elements interacting with the carpet floor.

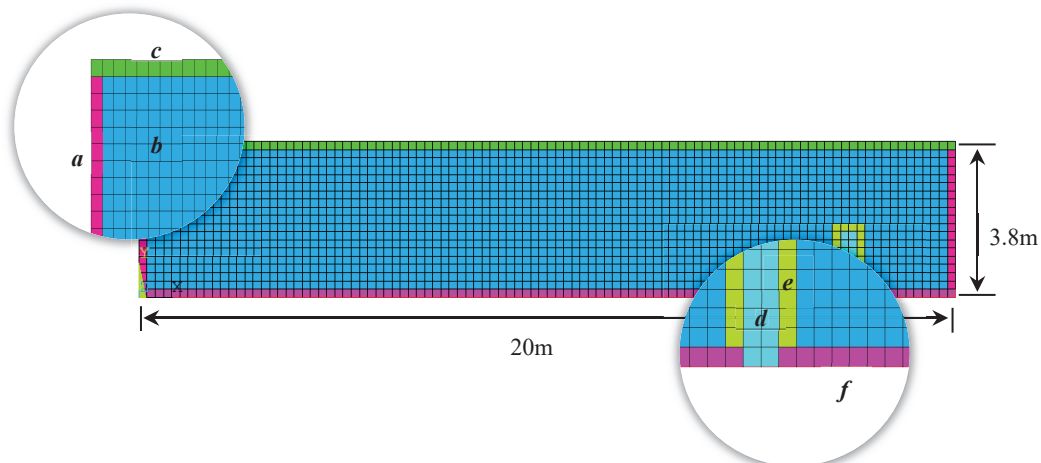


Figure 3 – 2D FE vibro-acoustic model showing element distribution (using low resolution mesh for clarity)

Besides the geometric data, the absorption coefficients for surface materials and the location of sound source was also modelled. The acoustic fluid elements require density and sonic velocity to be specified as material properties. Sound absorption exists at FSI, therefore specific boundary admittance (ζ) was also specified (13,26,27) at all FSI interfaces.

Table 1 – Material Properties

| Material | E (Pa) | ρ (kg/m ³) | ν | c (m/s) | ζ |
|-------------|-------------------|-----------------------------|-------|-----------|---------|
| Barrier | 1.8×10^9 | 680 | 0.22 | - | 0.025 |
| FSI Brick | - | 1.21 | - | 343 | 0.01 |
| FSI Ceiling | - | 1.21 | - | 343 | 0.015 |
| FSI Carpet | - | 1.21 | - | 343 | 0.025 |
| Air | - | 1.21 | - | 343 | - |

E = Young's Modulus, ρ = Density, ν = Poisson's ratio, c = Sonic velocity, ζ = damping

For structural elements, Young's modulus, density, Poisson's ratio, and material dependent damping

were specified. All material properties except the boundary admittance are as listed in Table 1. Other than the barrier element all others are fluid elements, FSI elements are air in contact with the respective surface and hence only absorption properties are required.

When the structure and fluid systems interact, a solution cannot be obtained without considering the coupled system. Accordingly, the simulation was executed using a real-time coupling between the structural and fluid elements accounting for FSI. Using this method, the surface absorption was modelled into the respective interface element and fluid properties into the fluid elements. This allows reducing the number of structural elements with displacement in UX and UY resulting in a computationally efficient model.

A harmonic analysis incorporating FSI was carried out using the ANSYS Parametric Design Language (APDL). Planar acoustic fluid elements along with 2D structural elements were used to model the vibro-acoustic system under consideration. Acoustic Fluid29 (28) elements were used to model the fluid part along with the companion Plane42 elements to build the structural part.

The acoustic elements that are in contact with the structural elements were modelled using Fluid29 unsymmetrical element matrix with UX, UY and pressure as the degrees of freedom. For modelling the inside fluid which is not directly in contact with the structural elements, Fluid29 with only pressure as a degree of freedom was used. Modelling the inside Fluid29 elements with only pressure was highly beneficial in terms of computational time, as the symmetric element matrices require less memory and can be executed efficiently.

2.2.1 Boundary Conditions

The displacements at all external walls were set to zero but allowing FSI. Fluid elements replicating the room air could resonate freely within the room boundary. In order to simplify the model and provide a uniform mesh, the barrier was represented as a single structural material. However, a two way FSI was enabled between the barrier and the surrounding air. Since the parameter of interest was the difference in SPL with and without the barrier, the sound source was modelled as a spherical vibration source mirroring the position of the experimental setup.

A mesh sensitivity analysis was carried out and found that the best results were obtained when the maximum element length (e_l) satisfied eight elements per wave length as shown in equation (3). The FE model was solved for a case with barrier and without barrier using an E5-2620 CPU at 2.1 GHz (12 CPUs) with 65536 MB RAM coupled with NVIDIA MAXIMUS setting coupling a Quadro K6000 and Tesla K20. The FEA model used in this work averages 172,674 nodes and 171,872 elements and takes 27 minutes to complete.

$$e_l = \frac{c}{8f} \quad (3)$$

3. RESULTS AND DISCUSSION

3.1 Experimental Test

The influence of a flat barrier 'F1' on the SPL of the test room under White and Pink noise are shown in Figure 4. With the barrier inserted, the SPL in the observation area reduced significantly. The SPL decreased for almost all frequencies at the one-third octave band. The highest reduction in SPL of 18.6 dB (White) and 15 dB (Pink) were observed at 16 kHz. The lowest reduction in SPL of 5dB (White) and 5.3dB (Pink) was observed for 160 Hz and 250 Hz respectively.

Comparing the performance of the barriers for White noise as shown in Figure 5, it can be seen that the curving of the barrier has a certain influence on the measured SPL values. The flat barrier F1 is the most commonly used free standing partition in open-plan office environments. Consequently, it was interesting to compare the performance of the other barriers to F1. Out of the four barriers tested F1 showed peak SPL values of 62.7 dB, 66.9 dB and 66.1 dB at 200 Hz, 250 Hz and 500 Hz respectively. However, on all other frequency starting from 200 Hz except for 400 Hz, the performance of barriers F1 and C1 were comparable.

At certain low frequencies (100 Hz, 125 Hz, 160 Hz and 400 Hz) barrier C1 exhibited worse performance compared to F1. The worst performance was at the lowest measured frequency of 100 Hz with a 4 dB increase in SPL compared to F1. According to Howard and Angus (29), the transition between wavelength being small and large with respect to the opening occurs when the opening size is about two thirds of the wavelength. Thus, considering that the room's height is 3.8m and the barrier

1.5m, below 98.5 Hz most of the sound will be diffracted. Considering this, it is worth investigating the influence of such shapes on low frequencies as low frequency noise is often hard to insulate against. However, for medium to high frequencies significant differences in the SPL values were not observed. This was reflected in the A-weighted single number quantity for White noise with LA_{eq} values for both partitions F1 and C1 at exactly 71.4 dB. This shows that the sound reductions exhibited by these two barriers were very similar for the test enclosure considered.

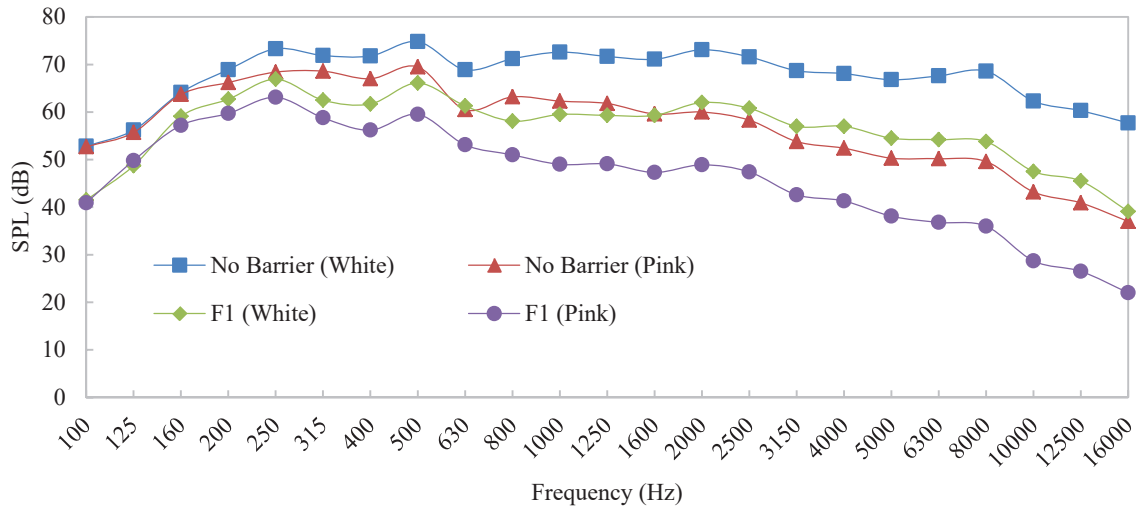


Figure 4 – Influence of barrier F1 on the measured SPL for White and Pink noise

On the other hand, barriers C2 and Z1 were found to exhibit slightly improved sound reduction performance compared to F1 for White noise. Inserting barrier C2, the measured SPL of the room decreased for almost all frequencies except for 100 Hz, 125 Hz and 800 Hz. The highest improvement was found to be at 250 Hz with a reduction in SPL of 5 dB. However, the worst performance was at the lowest measured frequency of 100 Hz with an increase in SPL of 2.2 dB. Overall the performance of C2 was slightly better than F1 with an overall LA_{eq} of 69.6 dB; an improvement of 1.8 dB compared to F1.

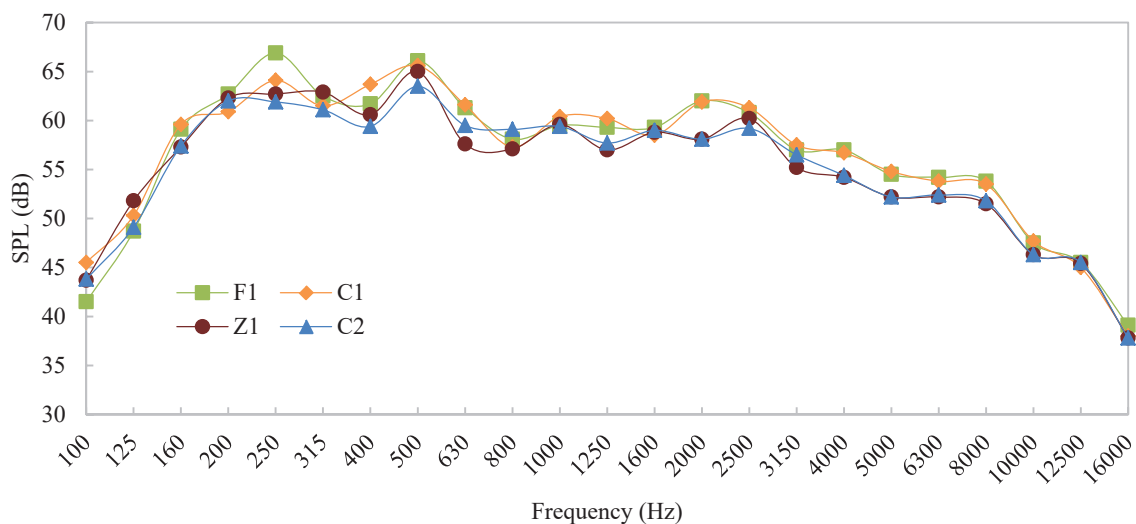


Figure 5 – Performance of the noise barriers tested under white noise

Barrier Z1 exhibited similar performance to C2, reducing the measured SPL values in the enclosure when exposed to white noise. Compared to F1, the highest improvement in performance of 4.2 dB was observed at a frequency of 250 Hz and the worst at 125 Hz with an increase in SPL of 3.1 dB. Except for 100 Hz, 125 Hz and 250 Hz, SPL of the room decreased for almost all other frequencies tested. This shows that similar to C2, design Z1 exhibits superior sound reduction performance

compared to F1 of similar dimensions. At the single number rating the performance of Z1 was very close to C2 with LA_{eq} of 69.7 dB exhibiting only 0.1 dB differences. However, this was an improvement of 1.7 dB compared to F1 for White noise.

Comparing the performance of the barriers for Pink noise as shown in Figure 6, it can be seen that the shape of the barrier has a certain influence on the measured SPL values. Out of the four barriers tested F1 showed peak SPL values of 63.1 dB and 59.5 dB at 250 Hz and 500 Hz respectively. However, on all other frequencies starting from 200 Hz except for 1000 Hz, the performance of barriers F1 and C1 were comparable.

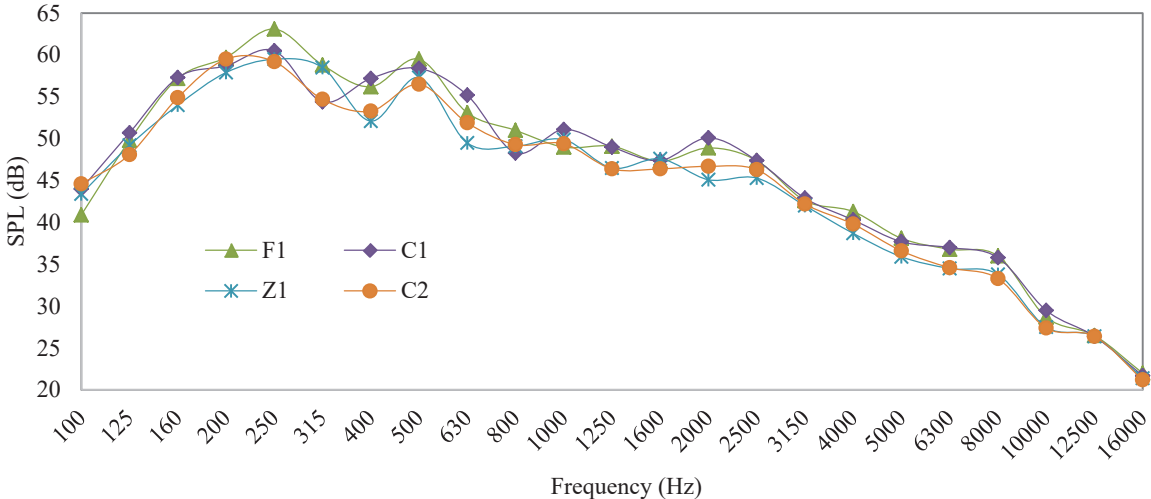


Figure 6 - Performance of the noise barriers tested under Pink noise

At 100 Hz and 1000 Hz, C1 exhibited worse performance compared to F1 by 3.1dB and 2.1 dB respectively. However, looking at Pink LA_{eq} values, C1 performed marginally better at 62.1 dB compared to F1 at 62.7, which is a difference of 0.6 dB. For pink noise, barrier C2 exhibited slightly improved acoustic insulation compared to F1.

Inserting C2, the SPL of the room decreased for almost all frequencies except for 100 Hz and 1000 Hz. The highest improvement was found at 250 Hz with a reduction in SPL of 3.9 dB. The worst performance was at the lowest measured frequency of 100 Hz with an increase in SPL of 3.7 dB. Overall the performance of C2 was better than F1 and C1 with an overall LA_{eq} of 60.4 dB. This is an improvement of 2.3 dB and 1.7 dB compared to F1 and C1 respectively. Even though the improvements are marginal for the test case considered, this can be expected to increase as the barrier height increases or the ceiling height decreases. Further tests will be conducted to validate this as part of the next stage of this research.

Z1 also exhibited similar performance to C2 reducing the measured SPL in the enclosure under Pink noise. Compared to F1, the highest improvement in performance of 3.8 dB was observed at a frequency of 2000 Hz and worst at 100 Hz with an increase in SPL of 2.5 dB. Except for these two frequencies, SPL of the room decreased for all other measured frequencies. At the single number rating the performance of Z1 was very close to C2 with LA_{eq} of 60.6 dB; this is an improvement of 2.1 dB and 1.5 dB compared to F1 and C1 respectively.

One of the possible explanations for the improvement being marginal can be the height of the ceiling/barrier. It is expected that if the same barriers were tested in a low height ceiling the sound reduction performance obtained due to added curvature may improve. However, further tests are necessary to study this aspect. Consequently, this would be one of the key aspects on the follow-on study. Furthermore, other possible versions of curvature need be studied as well to come up with an optimised curved design for best sound reduction.

3.2 Finite Element Analysis

Considering the purpose of the study was to analyse the influence of barrier shape (curved designs) on the SPL, it was deemed useful to develop a vibro-acoustic FE model incorporating FSI between barrier and the surrounding fluid (air). Using a simple 2D model two different scenarios were simulated; (i) a case with no barriers and (ii) a case which replicates the most common barrier used in

open-plan offices ‘F1’. Figure 7 presents the SPL obtained from the FE simulation in comparison with experimental measurements.

Comparing the SPL values, significant difference between the FEA results and experimental tests data were observed. However, this was expected as the sound source used for FEA was a frequency dependent vibration rather than a sound power. Consequently, the most important aspect here was to see whether the trend in SPL from FEA and experimental test were similar (no considering the actual numerical accuracy, i.e. dotted trend line in Figure 7).

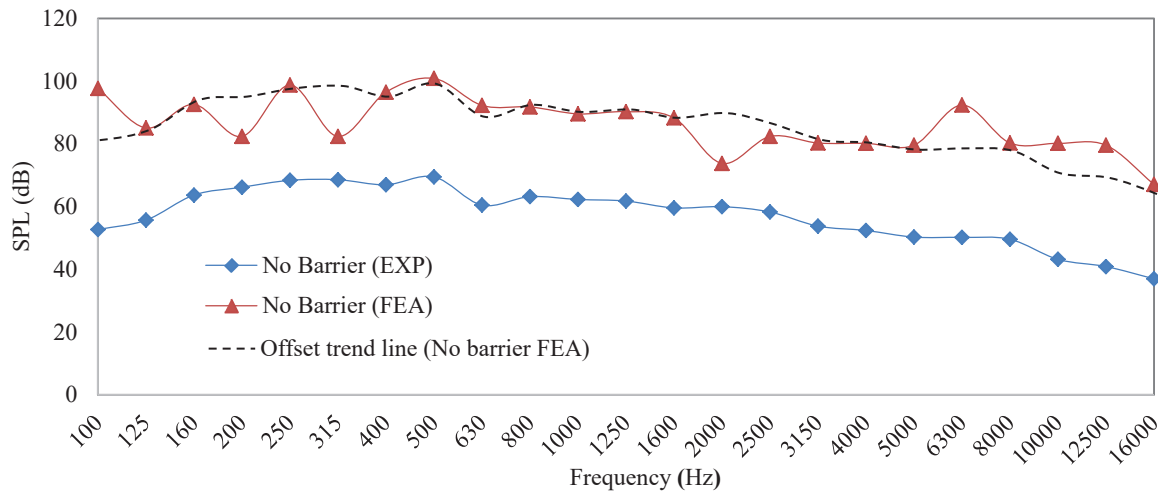


Figure 7 –Experimental and FEA measurements for enclosure with no barrier

Even though significant fluctuations in FEA values were observed between 100 Hz to 500 Hz, the FEA results exhibited a similar trend with respect to experimental except for 200 Hz and 6300 Hz as represented by the dotted trend line. The localised fluctuations in SPL can be due to the influence of eigen mode frequencies in relation to the geometry of the room.

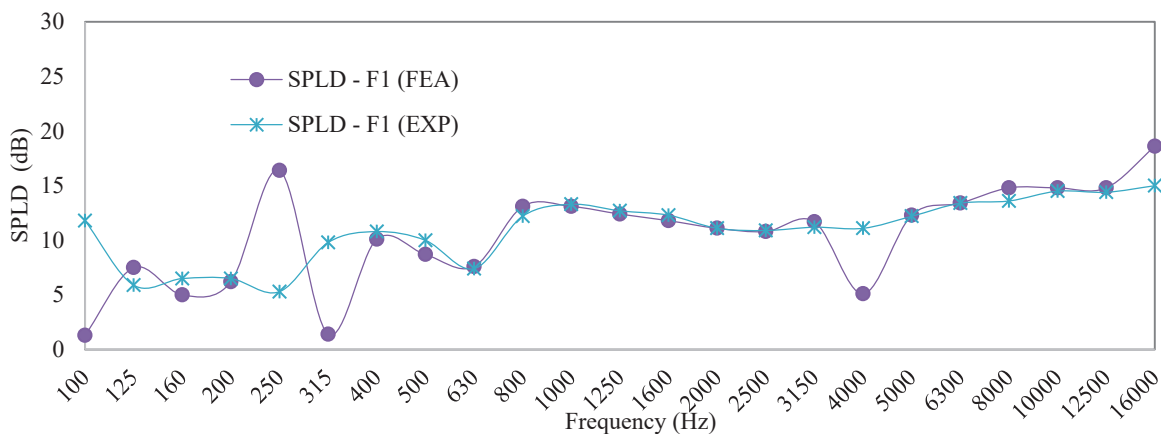


Figure 8 – FEA and Experimental comparison of SPLD after installation of barrier F1

Another important parameter to analyse the suitability of the FE model was to see whether the Sound Pressure Level Difference (SPLD) after barriers insertion were numerical comparable. Consequently, Figure 8 compares the SPL difference after installation of barrier F1 between FEA and experimental test. As can be seen, the FEA results closely follow the experimental measurement except for certain critical frequencies.

Difference between experimental and FEA of 11.1 dB at 250 Hz followed by 10.5 dB, 8.4 dB, 6 dB at 100 Hz, 315 Hz and 4000 Hz respectively were observed. Other than the influence of eigen modes the simplified 2D model used for the analysis can be another reason for this. Other than for these critical frequencies, the experimental and FEA results seems to agree closely. This is particularly encouraging and provides a new view point for classification of barrier shapes within an enclosed environment. There are also no published FSI model to demonstrate the influence of barrier shapes

within an enclosed environment.

In addition to the numerical SPL, it was also interesting to visualise the spatial acoustic distribution in the enclosure with and without the barrier. The SPL distribution at 400 Hz without the barrier can be seen on Figure 9(a) and 9(b) shows the influence of the barrier F1 on the SPL. Compared to the experimental test, FEA allows the SPL to be visualised. After the introduction of the barrier an increase in SPL on the source side and a reduction in receiving side can be observed. This can aid in optimising various aspects of the barrier and enclosure considering both the geometry of the room and barrier.

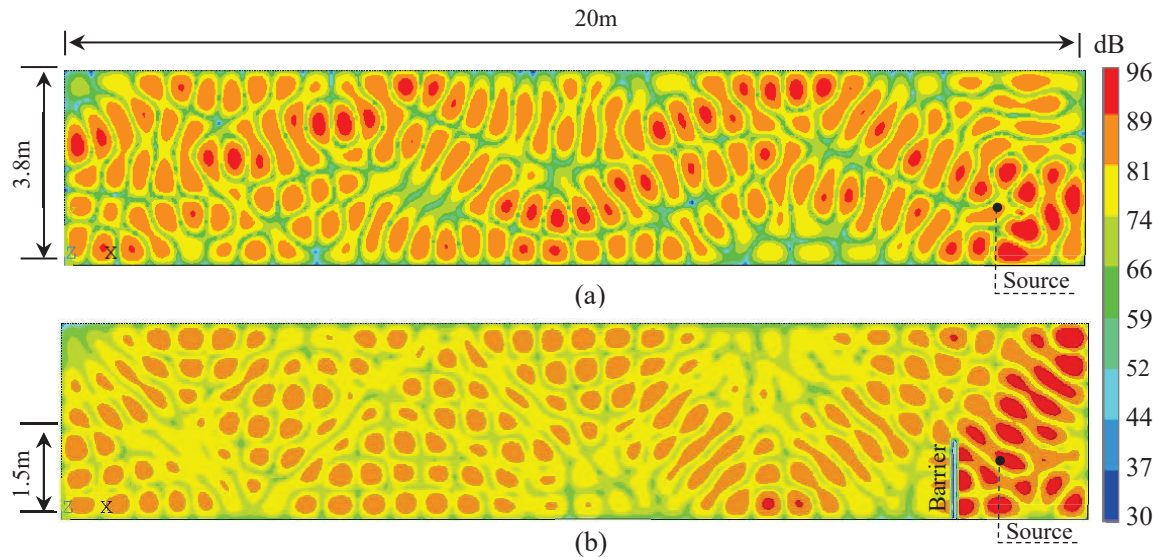


Figure 9 – Spatial SPL distribution at 400 Hz for (a) enclosure without barrier and (b) enclosure with barrier F1

Based on the results obtained, the 2-D FE modelling procedure presented in this work can be used to predict the acoustic performance of barrier in an enclosed environment. The FEA model presented is effective as it is a 2D approximation model and can be executed efficiently. The SPL performance of barriers can help designers to test the performance of various barrier designs before the need for being prototyped. This in turn can accelerate the development of sustainable and acoustically efficient open-plan areas.

4. CONCLUSION

The potential for using curved geometry to improve the acoustic performance of indoor barriers is investigated in this paper. As part of the study, a 2D numerical model featuring FSI between the barrier and the enclosed acoustic fluid is also developed using FEM. The performance of four different barriers were analysed in a typical enclosure and SPL values compared. Out of the four barriers tested, two designs C2 and Z1 showed reduction in SPL compared to the commonly used barrier F1 of similar global dimensions. C2 and Z1 exhibited highest reduction in SPL of 5 dB and 4.2 dB at 250 Hz when exposed to White noise. For pink noise, the highest reduction was 3.9 dB at 250 Hz for C2 and 3.8 dB at 2kHz for Z1. For C1 and Z1 improvements in SPL were observed for almost all frequencies resulting in an overall improved LA_{eq} values in comparison to F1.

Preliminary results comparing the SPLD between experimental and FEA results for F1 showed good agreement for all frequencies except for critical frequencies. The localised fluctuation was identified as the possible influence of Eigen modes or due to the simplified 2D model used. Using the FEA model the spatial SPL distribution was visualised showing effective FSI between the structural barrier and the enclosed fluid medium.

Despite valuable findings, it is acknowledged that continued analysis need to be carried out varying the ceiling/barrier height to further quantify the extent to which SPL improvements can be expected through curved designs. Consequently, a 3D FEA model will also be developed as part of the next stage of research.

REFERENCES

1. Lau SK, Tang SK. Performance of a noise barrier within an enclosed space. *Appl Acoust* 2009 1;70(1):50-57.
2. Kurze UJ, Anderson GS. Sound attenuation by barriers. *Applied Acoustics* 1971 January 1971;4(1):35-53.
3. Maekawa Z. Noise reduction by screens. *Applied Acoustics* 1968 July 1968;1(3):157-173.
4. Moreland JB, Minto RF. An example of in-plant noise reduction with an acoustical barrier. *Applied Acoustics* 1976 July 1976;9(3):205-214.
5. Huang X, Zou H, Qiu X. A preliminary study on the performance of indoor active noise barriers based on 2D simulations. *Build Environ* 2015 12;94, Part 2:891-899.
6. Shuo-Yen L, Sohei T, Sakae Y, Shinichi S. Improvement of sound transmission loss of double-layer wall by using vibration absorber. *Acoustical Science and Technology* 2014;35(2):119-121.
7. RL M, M T, D T. Improvement of sound insulation performance of double-panel structures by using damping materials . *Noise Control Engineering Journal* 2012;60:473-480.
8. Jagniatinskis A, Fiks B, Mickaitis M. Determination of Insertion Loss of Acoustic Barriers under Specific Conditions. *Procedia Engineering* 2017;187:289-294.
9. Sez nec R. Diffraction of sound around barriers: Use of the boundary elements technique. *Journal of Sound and Vibration* 1980 22 November 1980;73(2):195-209.
10. Li KM, Wong HY. A review of commonly used analytical and empirical formulae for predicting sound diffracted by a thin screen. *Appl Acoust* 2005 1;66(1):45-76.
11. Arjunan A, Wang CJ, Yahiaoui K, Mynors DJ, Morgan T, English M. Finite element acoustic analysis of a steel stud based double-leaf wall. *Build Environ* 2013 9;67:202-210.
12. Arjunan A, Wang CJ, Yahiaoui K, Mynors DJ, Morgan T, Nguyen VB, et al. Development of a 3D finite element acoustic model to predict the sound reduction index of stud based double-leaf walls. *J Sound Vibrat* 2014 11/24;333(23):6140-6155.
13. Arjunan A, Wang C, English M, Stanford M, Lister P. A Computationally-Efficient Numerical Model to Characterize the Noise Behavior of Metal-Framed Walls. *Metals* 2015;5(3):1414.
14. Arjunan A, Wang C, Yahiaoui K, Mynors M, Morgan T, Nguyen B, et al. Sound frequency dependent mesh modelling to simulate the acoustic insulation of stud based double-leaf walls. *Proceedings of the 2014 Leuven Conference on Noise and Vibration Engineering (ISMA2014)*. 2014.
15. Finite Element Vibro-acoustic Simulation of Roll-formed Steel Studs in Partition Walls. *Proceedings of the NAFEMS World Congress 2015; 21-24 June; San Diego, California, USA: NAFEMS; 2015*.
16. Fahy FJ, Gardonio P. *Sound and Structural Vibration: Radiation, Transmission and Response*. : Elsevier Science; 2007.
17. Dijkmans A. Wave based modeling of structure-borne sound transmission in finite sized double walls. *Proc.of Euronoise2015, Maastricht 2015*.
18. Mak CM, Wang Z. Recent advances in building acoustics: An overview of prediction methods and their applications. *Build Environ* 2015 9;91:118-126.
19. Takahashi D, Sawaki S, Mu R-. Improvement of sound insulation performance of double-glazed windows by using viscoelastic connectors. *J Sound Vibrat* 2016 6/9;371:56-66.
20. Papadopoulos CI. Development of an optimised, standard-compliant procedure to calculate sound transmission loss: design of transmission rooms. *Appl Acoust* 2002 9;63(9):1003-1029.
21. Papadopoulos CI. Development of an optimised, standard-compliant procedure to calculate sound transmission loss: numerical measurements. *Appl Acoust* 2003 11;64(11):1069-1085.
22. BS EN ISO 3382-3:2012. *Acoustics. Measurement of room acoustic parameters. Open plan offices*. 2012.
23. BS EN ISO 10140-1: *Acoustics. Laboratory Measurement of Sound Insulation of Building Elements. Application Rules for Specific Products*. 2014.
24. BS EN 61672-1:2013. *Electroacoustics. Sound level meters. Specifications*. 2013.
25. Norton MP, Karczub DG. *Fundamentals of Noise and Vibration Analysis for Engineers*. : Cambridge University Press; 2003.
26. Del Coz Díaz JJ, Álvarez Rabanal FP, García Nieto PJ, Serrano López MA. Sound transmission loss analysis through a multilayer lightweight concrete hollow brick wall by FEM and experimental validation. *Build Environ* 2010 11;45(11):2373-2386.

27. Sound Transmission Loss of Light-Weight Slotted Steel Studs in a Gypsum Plasterboard Partition Wall. InterNoise 2016; 2016.
28. ANSYS Acoustic guide: Theory reference, acoustics, acoustic fluid fundamentals. 2009.
29. David H, Jamie A. Acoustics and Psychoacoustics. 4th ed.: Focal Press; 2009.